JOURNAL OF AIRCRAFT
Vol. 30, No. 5, Sept.–Oct. 1993

Numerical Simulation of Unsteady Flow Induced by a Flat Plate Moving Near Ground

A. O. Nuhait* and M. F. Zedan†
King Saud University, Riyadh 11421, Saudi Arabia

An aerodynamic model based on the general unsteady two-dimensional vortex-lattice method and the method of images was developed to predict the unsteady ground effect on the aerodynamic characteristics of a flat plate. The wake is computed as part of the solution by allowing it to deform and roll up into its natural force-free position. The model is not restricted by angle of attack, sink rate, and camber. The results agree perfectly with available exact (steady) solutions. It is also shown that the increase in the magnitude of C_L and C_M as a result of unsteady ground effect is greater for high sink rates, in a general agreement with published results. On the other hand, the effect of ground on wake shape and position is greater for lower sink rates. For large sink rates, the wake becomes very close to the flight path with its position less dependent on the height above the ground.

Introduction

THE aerodynamic characteristics of an aircraft are known to be influenced by ground proximity during takeoff and landing. The interaction of the aircraft with the ground is known in the literature as "ground effect." This phenomenon is also observed in ship motion near a canal wall or near a second ship and in the motion of land-based vehicles. The extensive research conducted to understand and predict ground effect was motivated mainly by the fact that takeoff and landing are among the most dangerous phases of flight. The flow during these phases is inherently unsteady even if the aircraft is moving at constant velocity. This is attributed to the continuous change in the bound circulation around the wings as the ground is approached causing vorticity to be shed into the wake. Experimental studies of this unsteady phenomenon proved to be extremely difficult.

On the analytical side, the problem is too complicated to model a full aircraft; however, valuable insight can be obtained by considering the lifting surfaces. This can be further simplified by considering two-dimensional airfoils or even flat plates. Unfortunately, most of the previous investigators dealt with this unsteady flow situation in a quasisteady fashion. Basically, they tried to obtain the ground effects on the aerodynamic parameters (C_L and C_M) by solving the steady flow around an airfoil moving parallel to the ground at a fixed level (height). This solution is repeated at various heights; each time with an angle of attack equal to that of the airfoil approaching the ground at that height.

The accuracy of this steady simulation is not established yet. The work of Chen and Schweikhard[1] appears to be the only two-dimensional study to address the unsteady aspects of the problem. These aspects may be called unsteady (dynamic) ground effect. However, their results are limited and their approach does not seem to be rigorous in the treatment of the path of the wake.

The objective of the present study is to present a rigorous model to study the unsteady ground effect, in which the wake is properly considered by allowing it to deform and roll up into its natural force-free position which is calculated as part of the solution. It should be noted that the analysis is completely unsteady. Even when steady results are needed for comparison purposes, they are obtained by means of the unsteady solution using an impulsive start of an airfoil moving parallel to the ground.

Previous Work

The early studies on ground effect were analytic or semi-analytic and dealt with the steady problem. The tremendous improvements in computational hardware capabilities and in numerical techniques in recent years made it possible to study the unsteady ground effect for airfoils and finite wings.

Wieselsberger[2] was apparently the first to solve this problem. He used the method of images, thus satisfying the no-penetration boundary condition on the ground surface automatically. About 10 yr later, Tomotika et al.[3] used the conformal mapping technique to obtain the exact solution for the flow around a flat plate near ground. In 1935 Pistolesi[4] gave a comprehensive review of early work related to ground effect. Havelock[5] obtained an exact solution for the flow past an elliptic cylinder between two parallel plates by conformal mapping. Using a limiting process he obtained a series solution for the flow past a flat plate near a single wall (ground) which matched Tomotika's solution far from the wall. Green[6] obtained the solution for a circular-arc airfoil and later[7] for an airfoil with finite thickness near a plane wall also using conformal mapping. He showed that camber tends to increase the lift, while thickness tends to decrease it first and then increase it as the ground is approached. Based on the opposite effects of camber and thickness, one may expect the results of a flat plate in ground proximity to give a reasonable approximation for actual airfoils.

All the above studies, except Wieselsberger's were two-dimensional and all of them treated the problem by solving steady flow around the airfoil at fixed heights above ground. As mentioned, in the introduction Chen and Schweikhard[1] solved the unsteady (dynamic) problem for a flat plate in which the height above the ground varies continuously with time, but their solution had the shortcoming of assigning the wake along the flight path. They reported lift increases (as the ground is approached) greater than when the problem is treated as steady. Recently, ground effect for three-dimensional configurations was investigated. Katz[8] used a vortex-lattice method allowing the wake to deform freely to investigate the performance of a lifting surface close to the ground as found in racing cars. Chang[9] and Chang and Muirhead[10,11] experimentally investigated the steady and unsteady ground effects for flat delta wings. They reported an increase in the aerodynamic coefficients as the ground is approached in both cases; however, the increase was less in the unsteady problem

Received Aug. 23, 1991; revision received May 1, 1992, accepted for publication May 27, 1992.

*Chairman, Mechanical Engineering Department. Member AIAA.
†Associate Professor, Mechanical Engineering Department.

in contrast with the two-dimensional results of Chen and Schewikhard.[1] Recently, Nuhait and Mook,[12] Nuhait,[13] and Mook and Nuhait[14] used the vortex-lattice method, allowing the wake to deform freely, to study the unsteady ground effect for finite wings. When the height is measured by the level of the $\frac{1}{4}$-chord point above the ground, their results indicated that increases in aerodynamic coefficients are weakened in the unsteady problem in agreement with Chang[9] and Chang and Muirhead.[10,11] Clearly the general three-dimensional problem of the ground effect is quite complicated and involves too many parameters to make any study universal. The present authors believe that a good understanding of the two-dimensional problem, when considered properly, may be of great benefit at the present time. Such proper handling of the unsteady two-dimensional problem appears to be lacking in the literature. The objective of this article is to provide such a solution for this problem with minimum or no approximations.

Method of Analysis

The flow is assumed to be two-dimensional, incompressible, and inviscid. Following Wieselsberger,[2] we simulate the ground effect by placing the image of the real plate and its starting vortex (wake) below the ground plane as shown in Fig. 1. The present method is based on a flat plate moving through the air instead of the air blowing over the plate. Two reference frames are used; one is fixed to the ground (*G-F*) and the other is fixed to the body (*B-F*), as shown in Fig. 2. Other definitions are given in the figure.

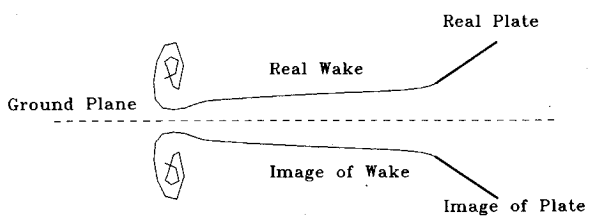

Fig. 1 Plate and its wake and their images.

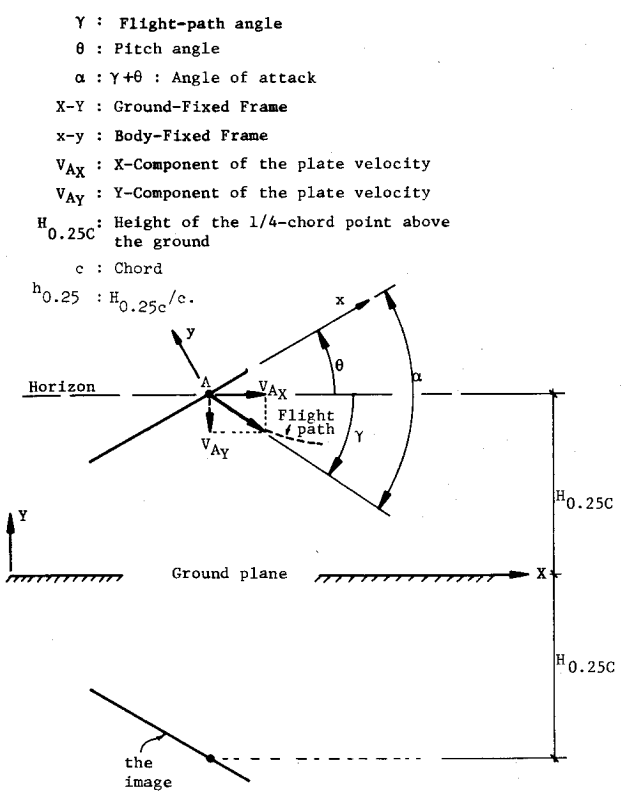

Fig. 2 Two coordinate systems: ground-fixed (*G-F*) frame and body-fixed (*B-F*) frame.

Basic Equations

The plate, its wake, and their images are represented by sheets of vorticity. The sheet representing the plate has its position specified and is called a "bound vortex sheet"; a pressure jump may exist across it. The sheet representing the wake, whose position is not known in advance, deforms freely and assumes a force-free position during the simulation. As a result, it is called a "free vortex sheet" and a pressure jump cannot exist across it. The bound and free vortex sheets are joined along the trailing edge of the plate. The two vortex sheets are replaced with discrete vortices. The total velocity field induced by these vortices must satisfy the continuity equation and the conditions: 1) $V_{\text{disturbance}} \to 0$ at infinity; 2) the vertical velocity component is zero on the ground plane; 3) the no-penetration condition is satisfied on the plate; 4) the total circulation around a closed fluid line around the plate and its wake is conserved (zero in this case); 5) the so-called unsteady Kutta condition is satisfied at the trailing edge of the plate; and 6) the pressure is continuous in the wake.

Before proceeding further, we write all variables in dimensionless form by introducing the characteristic variables: the speed characterizing the motion of the plate U, the physical length of a bound element l, and the characteristic time l/U. The dimensionless variables are as follows:

$$V = \frac{V^*}{U}, \quad w = w^* \frac{l}{U}, \quad \phi = \frac{\phi^*}{Ul}$$

$$r = \frac{r^*}{l}, \quad P = \frac{P^*}{\rho^* U^2}, \quad t = t^* \frac{U}{l}$$

where V, w, ϕ, r, P, and ρ denote velocity, angular velocity, velocity potential, position vector, pressure, and density, respectively. The asterisk denotes the physical quantities.

The velocity induced by the discrete vortices is computed by using the Biot-Savart law. As a result, the continuity equation and the first of the conditions stated previously are satisfied. Because the method of images is used the ground is a plane of symmetry, and therefore, the second condition is satisfied too. The third condition is written simply as

$$(V - V_p) \cdot n = 0 \tag{1}$$

where V is the absolute velocity of a fluid particle, n is a unit vector that is normal to the plate, and V_p is the absolute velocity of a point on the plate in contact with the fluid particle. V_p is given by

$$V_p = V_A + w \times r_p + (\delta r_p/\delta t) \tag{2}$$

in which V_A is the linear velocity of the plate at point A (Fig. 2); w is its angular velocity; r_p is the position vector of point p with respect to point A, and $\delta r_p/\delta t$ is the local velocity of point p with respect to point A. The plate is considered rigid, hence, $\delta r_p/\delta t$ is equal to zero. Also, w is assumed zero. Therefore, V_p is equal to V_A. This means that all points on the plate have the same velocity. The plate is discretized into $(N - 1)$ equal length panels (elements). The vorticity on each element is considered to be uniform and is replaced by one-point vortex of strength Γ located at a distance equal to $\frac{1}{4}$ of the element length behind its leading edge, as shown in Fig. 3.

Following Mook et al.[15] we simulate the starting vortex by placing a vortex core with unknown strength (Γ_c) at a point $l/4$ behind the plate trailing edge (Fig. 3). As the number of elements increases, the location of the first-point vortex will approach the plate leading edge, and the location of the starting vortex will approach the plate trailing edge. The no-penetration boundary condition is imposed at one point (called a "control point") on each element located at a distance equal to $3l/4$ behind the leading edge of the element. With the above considerations in mind, and assuming the location and strength of the wake cores have been computed (the computation of

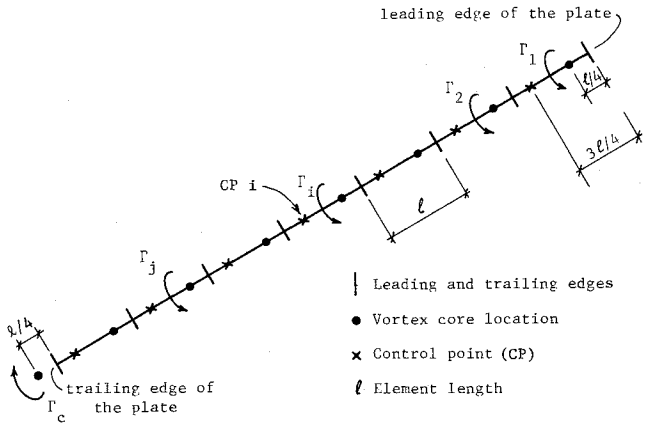

Fig. 3 Discretization of the plate.

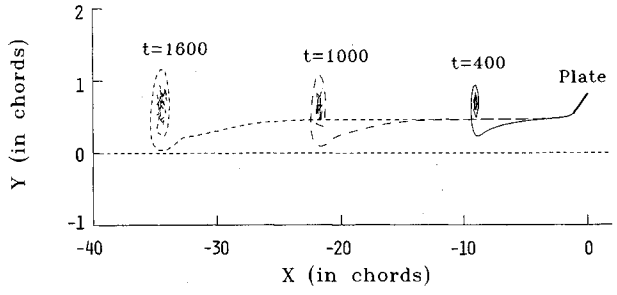

Fig. 4 Actual computed wake; starting vortex is shown at various time levels.

these at various time levels is discussed later), we can write Eq. (1) as

$$\sum_{j=1}^{N-1} A_{ij}\Gamma_j - Q_i\Gamma_c = (V_A - V_{wi})\cdot n_i \quad \text{on the plate for } i = 1, 2, \ldots, N-1 \tag{3}$$

in which the influence matrix element A_{ij} represents the normal velocity component induced at a control point i by the vortex core (having a unit circulation) of element j and its image. In general, the elements A_{ij} are functions of space and time. Γ_j is the unknown circulation of the vortex of element j. Q_i represents the normal velocity component induced at control point i by the starting vortex having a unit circulation and its image. V_{wi} is the velocity induced by the wake vortex cores and their images whose positions and circulations are known. At the moment motion begins V_{wi} is zero.

The fourth condition (total circulation around a closed fluid line must be conserved) is dictated by Kelvin's theorem. Since the total circulation was zero at the beginning of motion, then it will continue to be zero for a path that contains the same fluid particles. This condition can be written as

$$\sum_{j=1}^{N-1} \Gamma_j - \Gamma_c = \sum_{k=1}^{NT-1} \Gamma_{\text{wake}_k} \tag{4}$$

where NT is the number of time steps. Γ_{wake_k} is the circulation of a wake core at node k, which is zero at the start of motion. The fifth condition (unsteady Kutta condition) is satisfied by shedding the vorticity generated at the plate trailing edge (Γ_c) at the local fluid particle velocity. The wake is created as a result of shedding and convecting the starting vortex at each time step as shown in Fig. 4.

The sixth condition (pressure is continuous in the wake) is satisfied by convecting the wake cores at the local fluid particle velocity as required by the Kelvin-Helmholtz theorem (Konstadinopoulos[16]). This local fluid particle velocity is computed according to Eq. (2) with $w = 0$. The local fluid particle velocity simply becomes

$$(\delta r/\delta t) = V - V_A \tag{5}$$

where V is the absolute velocity induced by all the discrete vortices (bound and free) and their images. The new position of wake core k is computed by using the Euler method. That is

$$r_k(t + \Delta t) = r_k(t) + (\delta r/\delta t)_k \Delta t \tag{6}$$

where r_k is the position of the wake node core and Δt is the time step by which the solution is advanced.

Numerical Procedure

In order to solve Eqs. (3) and (4), an initial condition describing the wake (position and vorticity) must be prescribed. One special case of interest is when the plate is put into motion impulsively. At this instant no wake exists; hence, V_{wi} is zero, and Eqs. (3) and (4) reduce to

$$\sum_{j=1}^{N-1} A_{ij}\Gamma_j - Q_i\Gamma_c = V_A\cdot n_i \quad \text{for } i = 1, 2, \ldots, N-1$$
$$\sum_{j=1}^{N-1} \Gamma_j - \Gamma_c = 0 \tag{7}$$

Equation (7) is solved for the unknown circulations by Gaussian elimination. At the beginning of the first step ($NT = 1$) all the circulations in the bound and free vortex sheets are zero. At the end of this step, all the bound circulations have changed and a starting vortex is generated at the trailing edge. At the beginning of the second time step ($NT = 2$) in order to satisfy the unsteady Kutta condition, the trailing edge (starting) vortex is shed and convected downstream at the local particle velocity [Eq. (5)]. Its new position is computed by using Eq. (6), and in order to guarantee the temporal conservation of circulation, its circulation is set equal to the circulation of the starting vortex at $NT = 1$. The wake is created as a result of shedding and convecting the trailing-edge vortices. The bound circulations are calculated at the end of the second time step by using Eqs. (3) and (4) including the effects of the wake and its image. A second starting vortex is generated at the trailing edge and is then shed and convected downstream to its new position as required by the unsteady Kutta condition. Simultaneously, the first trailing-edge vortex is convected to its new position. The wake is growing. The bound circulations are computed at the end of the third time step. A third vortex forms at the trailing edge. The procedure for finding the solution of Eqs. (3) and (4) is repeated for any desired number of time steps. In Fig. 4, an actual computed wake for a flat plate at $\alpha = 14$ deg near the ground is shown for demonstration purposes.

Computation of the Aerodynamic Loads

The normal force and pitching moment are computed after the pressure-jump distribution is found. The pressure jump across each element is computed at the control point of that element by using the unsteady Bernoulli's equation. The pressure-jump coefficient at control point i, ΔCp_i, takes the following form:

$$\Delta Cp_i = (C_{pl} - C_{pu})_i = 2\frac{\partial}{\partial t}(\phi_u - \phi_l)_i + (V_u - V_l)_i\cdot(V_u^+ V_l - 2V_{A_x})_i \tag{8}$$

in which the u and l denote the upper and lower surfaces, respectively, ϕ is the velocity potential expressed in terms of the body-fixed frame, V_{A_x} is the x component of the plate velocity in terms of the body-fixed frame.

The quantity $(\phi_u - \phi_l)_i$ is evaluated by integrating the velocity along a path that starts just above the control point i, goes upstream all the way around the leading edge, and then comes back downstream to just below the same control point. The following simple result is obtained:

$$(\phi_u - \phi_l)_i = \sum_{k=1}^{i} \Gamma_k$$

The term $(\partial/\partial t)(\phi_u - \phi_l)_i$ can be approximated by

$$\frac{\partial}{\partial t}(\phi_u - \phi_l)_i \simeq \left\{\left[\sum_{k=1}^{i} \Gamma_k(t + \Delta t) - \sum_{k=1}^{i} \Gamma_k(t)\right] \Big/ \Delta t\right\} \quad (9)$$

The right side of Eq. (9) is evaluated by storing the values of Γ_i for two successive time steps. V_u and V_l can be written in terms of the mean velocity V_m and the velocity jump γ as follows:

$$\begin{aligned} V_u &= V_m + (\gamma/2) \\ V_l &= V_m - (\gamma/2) \end{aligned} \quad (10)$$

V_m is the velocity induced by all the discrete vortices of the plate and its wake and their images at the control point.

From Eq. (10), γ and V_m are given by

$$\begin{aligned} \gamma &= V_u - V_l \\ 2V_m &= V_u + V_l \end{aligned} \quad (11)$$

The velocity jump γ is evaluated using the relation

$$\gamma_i = \{[(\text{Factor})\Gamma_i + \Gamma_{i+1}]/2l\} \quad (12)$$

in which "Factor" takes the value of 1, except for the first element it takes the value of 2. Substitution of Eqs. (9), (11), and (12) into Eq. (8), the pressure jump ΔCp_i becomes

$$\Delta Cp_i = \left(\left\{2\sum_{k=1}^{i}[\Gamma_k(t + \Delta t) - \Gamma_k(t)]\right\} \Big/ \Delta t\right) + \{[(\text{Factor})\Gamma_i + \Gamma_{i+1}]/l\}(V_m - V_{A_x}) \quad (13)$$

Once the pressure jump is known across all panels, the calculation of the normal force and the pitching moment by simple integration becomes straightforward. Standard definitions are used to calculate their coefficients (C_N, C_L, and C_M).

Results and Discussion

The method described in the previous section has been programmed and run on the IBM 370 3083 JX of King Saud University. The dimensionless time step (Δt) by which the solution is advanced in time was taken initially as 1; physically this is equal to the time required to travel a distance equal to one panel length at the freestream (reference) velocity. To get a feel for the program performance, it was run for a plate impulsively started very far from the ground (no ground effect) with a flight-path angle $\gamma = 0$ and an angle of attack $\alpha = 10$ deg. Figure 5 shows that the normal force coefficient C_N obtained increases monotically with time towards an asymptotic (steady) value. A preliminary run was made with $NT = 900$. At the last point in this run ($NT = 900$). $C_N = 1.04$. The exact steady value for this case is 1.07. Apparently, longer time ($NT > 900$) is needed to reach the steady value.

Selection of N_{core} and Δt

Running the program for a longer time is quite costly, because under normal conditions the number of vortex cores (N_{core}) shed into the wake is equal to the number of time steps (NT). However, at large values of NT, some of the vortices shed earlier are expected to be too far away in the wake to have any noticeable effect on the flow around the plate. Therefore, to save computer time and storage, it was decided to limit the number of cores by truncating the early ones once they are far enough from the plate; truncation is done once the number of cores reaches a certain preset value. To study the effect of truncation, the program was run up to $NT = 1100$ once without truncation, and another time with the number of cores truncated at 900 for a plate far from the ground. The results are shown in Fig. 5. A small jump is noticed at $NT = 900$ (which corresponds to the N_{core} kept). We concluded that all the vortices shed earlier in the wake still have a significant effect and $NT = 1100$ (which corresponds to $t = 1100$ in this case) is not enough to reach a steady condition. To avoid long computer run times, we doubled the time step ($\Delta t = 2$) and later tripled it while N_{core} was truncated at different values. This was done in a systematic way when the plate was far from the ground, and was repeated when the plate was impulsively started with the height of the ¼-chord point equal to $0.5c$ ($h_{0.25} = 0.5$) with $\gamma = 0$. Increasing the time step for a given number of cores substantially reduced the jump in C_N. Increasing the number of cores for a given time step had a similar effect when the airfoil was far from the ground and a negligible effect when close to the ground. Based on these results we concluded that choosing $\Delta t = 2$ and $N_{core} = 1100$ (which correspond to $t = 2200$) is expected to provide excellent results.

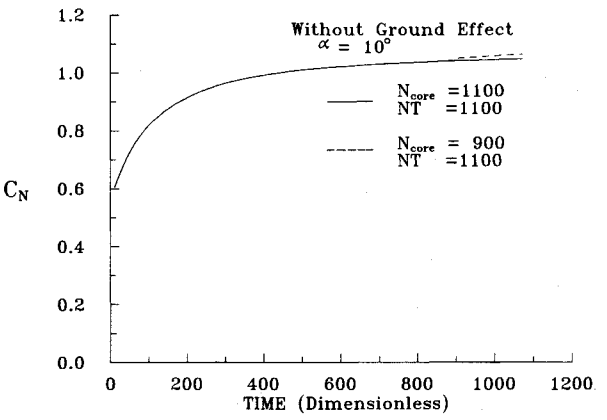

Fig. 5 Effect of truncation of early shed vortex cores on C_n for a plate far from the ground at $\alpha = 10$ deg using $\Delta t = 1.0$.

Validation of the Method

There are no exact solutions available for the unsteady ground effect to compare with. However, a reasonably good check on the method is made by comparing the steady results obtained by the present unsteady model and the analytic solutions of Tomotika et al.[3] and Havelock.[5] In the present runs, the plate is impulsively started to move at an angle of attack α parallel to ground at a fixed height (i.e., $\gamma = 0$) until steady flow is established as indicated by the constancy of C_N and C_M with time. The exact results of Tomotika et al. were picked up very carefully from a graph in Ref. 4 and tabulated as $(C_L - C_{L\infty})/C_{L\infty}$ vs $h_{0.5}$ for various values of α, where C_L and $C_{L\infty}$ are the steady lift coefficients with and without ground effect at the same α, and $h_{0.5}$ is the height of ½-chord point above the ground (as used in Ref. 4). Figure 6 shows almost perfect agreement between the exact solution and the present results for all values of α (up to 36 deg), and for $h_{0.5} = 0.20$–4.0. Chen and Schweikhard[1] also used Tomotika's (steady) results to validate their unsteady model, however, they reported some differences, especially at small h and large α. The series expansion of Havelock, as given by Plotkin and Kennell[17] which converges very fast for $h_{0.5} > 1$, was also used for comparison. We found that $\Delta C_L/C_{L\infty}$ obtained from this series was almost identical to the present results as well as to Tomotika's solution, and therefore, is not shown in Fig. 6. In fact, the series

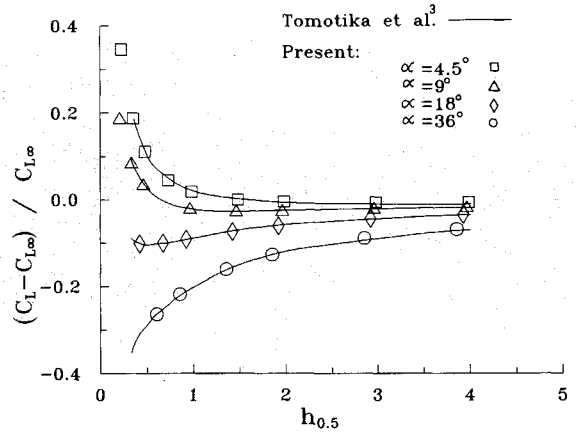

Fig. 6 Comparison between the steady results of the present model and the exact solution of Tomotika; γ = 0 deg.

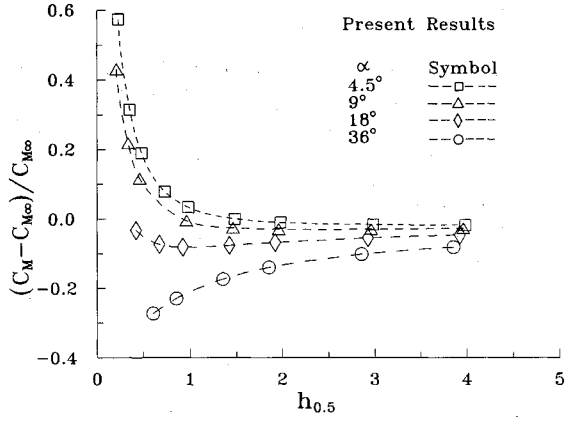

Fig. 7 Steady ground effect on moment coefficient (about leading edge); γ = 0 deg.

expansion of Tomotika's solution[4] for $h_{0.5} > 1$ can be shown to be identical to Havelock's expansion by using simple, but somewhat lengthy, algebraic manipulations.

The results for the deviation in the steady moment coefficient around the leading edge $(C_M - C_{M\infty})/C_{M\infty}$ as obtained from the present model shown in Fig. 7 are similar to the corresponding lift results; however, the effect of the ground on C_M seems higher at small angles of attack. We note that no exact results are shown because none is available to us; the dashed lines are simply curve fits of the results.

Unsteady Ground Effect on Aerodynamic Coefficients

The present model was run for a plate impulsively started far enough from the ground such that steady flow is established long before ground effect becomes noticeable. Typical results for the normal force coefficient C_N are shown in Fig. 8. We note that h in this figure, and from this point on, is measured from the $\frac{1}{4}$-chord point. Since we are interested in ground effects, we will concentrate on a small region in such plots near ground ($h_{0.25} \leq 4$), and the deviation of C_L is presented instead of C_N. In these computations the effects of the sink rate are obtained by varying the flight-path angle γ. Results are also compared with those of Chen and Schwiekhard.[1]

In Fig. 9 we show such a comparison for α = 2, 6, 10, and 14 deg. In order to compare with Chen and Schweikhard,[1] the results are presented for two values of γ (30 and 10 deg), and for γ = 0 deg which represents steady ground effect. For γ = 10 deg and for γ = 0 deg, the agreement is not bad (except very close to ground) for all values of α, which indicates that C_L increases as the ground is approached. However, the increase in unsteady ground effect is larger than the increase in the steady case. For γ = 30 deg the two studies

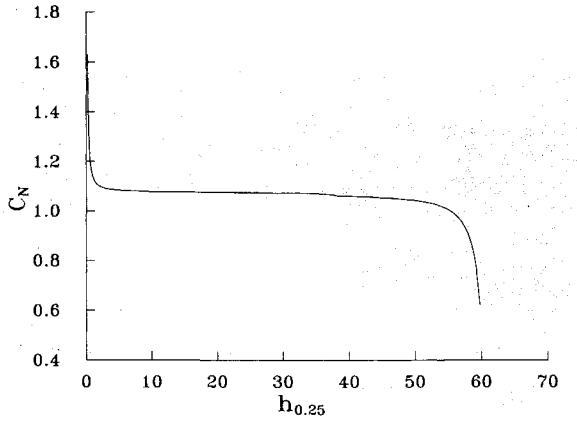

Fig. 8 Unsteady ground effect on normal force coefficient of a plate approaching the ground with γ = 30 deg at α = 10 deg.

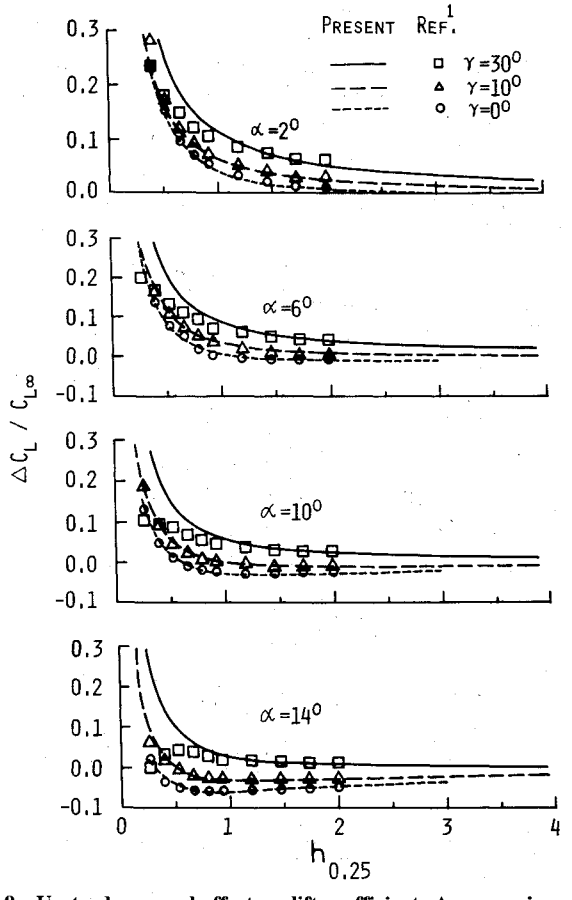

Fig. 9 Unsteady ground effect on lift coefficient. A comparison for α = 2, 6, 10, and 14 deg is shown.

agree far from ground, but differ progressively as the ground is approached; in fact, they disagree clearly very closely to the ground. The present results indicate a trend similar to that observed at γ = 10 deg at all values of α considered, whereas, the results of Chen and Schweikhard indicate a smaller rate of increase in $\Delta C_L/C_{L\infty}$ for α = 2, 6, and 10 deg, and a decrease for α = 14 deg. Their assumption of known wake position may be the reason for this behavior. This assumption may be acceptable far from the ground but not close to the ground.

Figure 10 shows the relative deviation of C_M from $C_{M\infty}$ for the cases presented in Fig. 9. The trends are generally similar to those of $\Delta C_L/C_{L\infty}$ in that the ground causes the magnitude of C_M to increase, and the increase is higher in the unsteady case than in the steady one except for α = 14 deg and γ = 10 deg for $h_{0.25} > 1.0$ (Fig. 10).

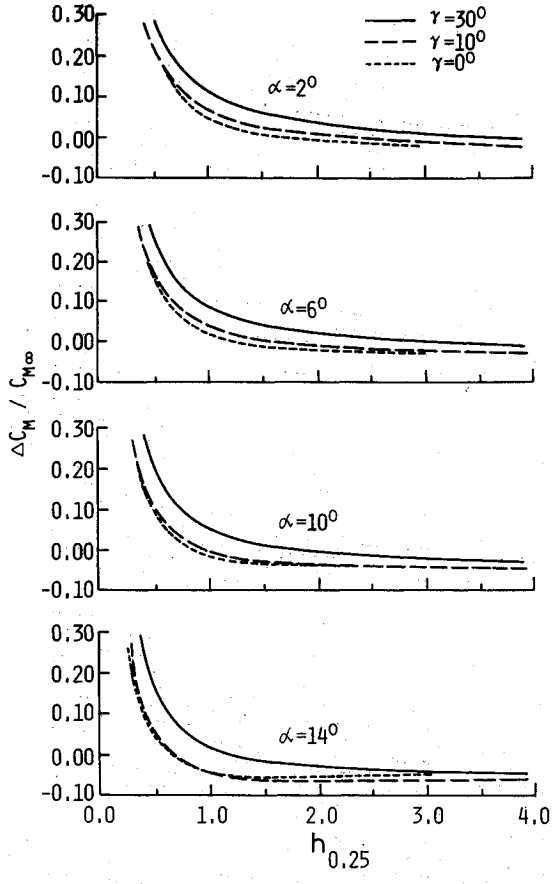

Fig. 10 Unsteady ground effect on moment coefficient (around leading edge). A comparison for α = 2, 6, 10, and 14 deg is shown.

Unsteady Ground Effect on Wake

The wake position was computed as discussed earlier and updated after each time step as the solution progressed. In Fig. 11 we show the wakes in the ground-fixed coordinate system, computed after 200, 500, and 800 time steps very far from ground, and at $h_{0.25}$ = 0.75 with α = 14 deg and γ = 0. In both cases, the plate was impulsively set into motion. To show the effect of the ground, the plate in the case with no ground effect was set above an imaginary ground at $h_{0.25}$ = 0.75. The figure indicates that the free vortex sheet of the wake (as represented by discrete cores) rolls up in both cases; the roll-up intensifies and its region is convected downstream as time progresses. However, the downward deflection of the sheet (wake) is much higher when no ground is present; in fact, it crosses the imaginary ground as shown in the upper part of Fig. 11. In contrast, when ground effect is considered the, force-free position of the wake is always above ground (as expected physically), although the rolled-up part comes very close to it far downstream of the plate.

In Fig. 12 we show the progress of wake position as the ground is approached at an angle of attack of 14 deg. In Fig. 12a we show the wake position of a plate impulsively started at values of $h_{0.25}$ = 0.25, 1.0, 4, and ∞, while moving parallel to the ground (γ = 0). This case is presented to serve as reference for the other two cases where the plate moves towards ground ($\gamma \neq 0$). In this figure we note that the wake is shifted in a way to make the plate identical for all values of h; therefore, the vertical coordinate should not be interpreted as level above ground. The results in Fig. 12a indicate (as expected) that ground effect on the wake increases as h decreases; in fact for $h_{0.25} \leq 1$ the wake (excluding the roll-up part as well as the part near the trailing edge of the plate) becomes almost parallel to the ground. Figure 12b shows the progress of the wake for a plate approaching the ground at a sink rate corresponding to γ = 10 deg. Steady conditions are

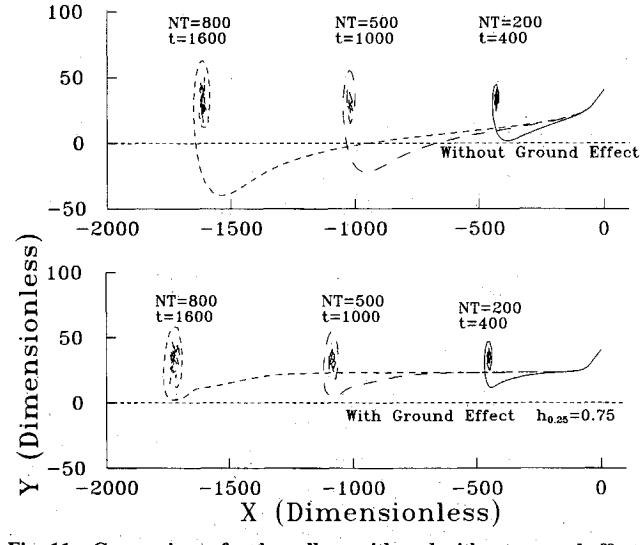

Fig. 11 Comparison of wake roll-up with and without ground effect; γ = 0 deg and α = 14 deg.

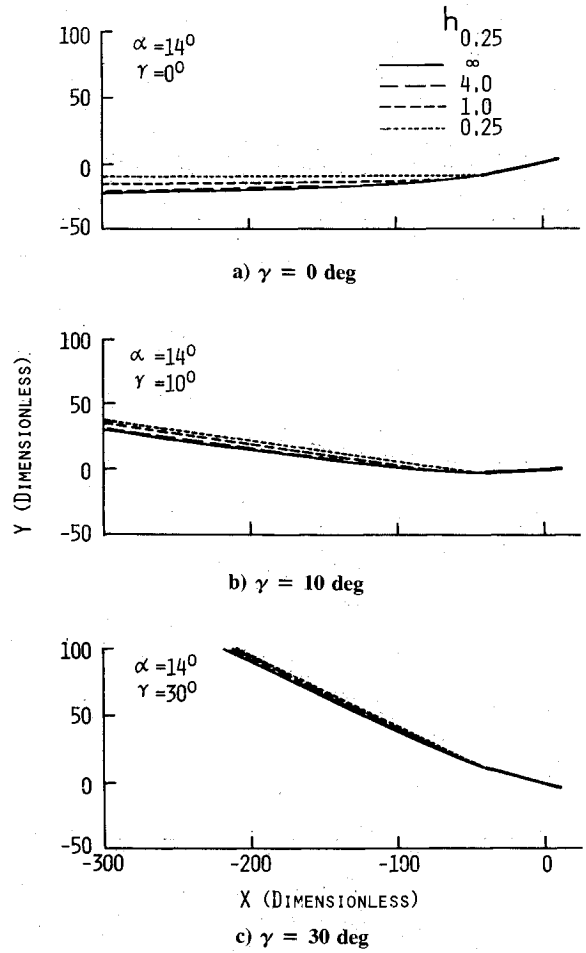

Fig. 12 Unsteady ground effect on wake shapes at various heights from the ground for α = 14 deg with different sink rates.

established very far from the ground, therefore, the differences in the wake positions at various heights are caused only by unsteady ground effects. The results indicate that the ground causes the wake to be displaced away from it compared to the case with no ground effect. However, such a displacement effect is not as dramatic as in the case with γ = 0. Again, this is expected because of the flight path. For the highest sink rate investigated (γ = 30 deg), the effect of ground on the wake becomes slightly weaker as shown in Fig. 12c.

Summary and Concluding Remarks

A numerical model has been developed to predict the unsteady ground effect on the aerodynamic characteristics of a flat plate as it approaches the ground. As in previous work, the effect of the ground is simulated by placing the plate image below ground surface. However, the wake is allowed to deform and roll up into its natural force-free position which is calculated as part of the solution. The method was calibrated by using extensive sensitivity studies and comparisons with available exact steady solutions. Steady results obtained by the present unsteady model agreed nearly perfectly with the exact solution for a wide range of h and α.

Case studies showed that the increase in the magnitude of C_L and C_M as ground is approached with $\gamma = 10$ and 30 deg is greater than in the corresponding increase in steady ground effect. This trend agrees with the results of Chen and Schweikhard except very close to the ground for $\gamma = 30$ deg at relatively large values of α. The results showed that the effect of ground on wake shape and position is greater at small values of h and γ (as expected). For larger sink rates, the wake becomes very close to the flight path with its position less dependent on h.

Acknowledgment

The authors wish to thank the staff of King Saud University Computer Center for their cooperation and help. Special thanks are due to the Director of the Center, Mohamed Al-Turaigi and also to Saif Al-Saab and Umit Dericioglu.

References

[1]Chen, Y.-S., and Schweikhard, W. G., "Dynamic Ground Effects on a Two-Dimensional Flat Plate," *Journal of Aircraft*, Vol. 22, No. 7, 1985, pp. 638–640.

[2]Wieselsberger, C., "Wing Resistance Near the Ground," NACA TM 77, April 1922.

[3]Tomotika, S., Nagamiya, T., and Takenouti, Y., "The Lift on a Flat Plate Placed Near a Plane Wall, with Special Reference to the Effect of the Ground Upon the Lift of a Monoplane Aerofoil," Aeronautical Research Inst., Rept. 97, Tokyo Imperial Univ., Tokyo, Aug. 1933 (as reported in Pistolesi, 1935).

[4]Pistolesi, E., "Ground Effect—Theory and Practice," NACA TM 828, July 1935.

[5]Havelock, T. H., "The Lift and Moment on a Flat Plate in a Stream of Finite Width," *Proceedings of the Royal Society of London*, Series A, Vol. 166, London, 1938, pp. 178–196.

[6]Green, A. E., "The Forces Acting on the Circular-Arc Aerofoil in a Stream Bounded by a Plane Wall," *Proceedings, London Mathematical Society*, Vol. 46, No. 2, London, 1940, pp. 19–54.

[7]Green, A. E., "The Two-Dimensional Aerofoil in a Bounded Stream," *Quarterly Journal of Mathematics*, Vol. 18, 1947, pp. 167–177.

[8]Katz, J., "Calculation of the Aerodynamic Forces on Automotive Lifting Surfaces," *Journal of Fluids Engineering*, Vol. 107, Dec. 1985, pp. 438–443.

[9]Chang, R. C., "An Experimental Investigation of Dynamic Ground Effect," Ph.D. Dissertation, Dept. of Aerospace Engineering, Univ. of Kansas, Lawrence, KS, April 1985.

[10]Chang, R. C., and Muirhead, V. U., "Investigation of Dynamic Ground Effect," *Proceedings of the 1985 NASA Ground Effects Workshop*, NASA CP-2462, 1985, pp. 363–391.

[11]Chang, R. C., and Muirhead, V. U., "Effect of Sink Rate on Ground Effect of Low-Aspect-Ratio Wings," *Journal of Aircraft*, Vol. 24, No. 3, 1987, pp. 176–180.

[12]Nuhait, A. O., and Mook, D. T., "Numerical Simulation of Wings in Steady and Unsteady Ground Effects," *Journal of Aircraft*, Vol. 26, No. 12, 1989, pp. 1081–1089.

[13]Nuhait, A. O., "Numerical Simulation of Feedback Control of Aerodynamic Configurations in Steady and Unsteady Ground Effects," Ph.D. Dissertation, Dept. of Engineering Science and Mechanics, Virginia Polytechnic Inst. and State Univ., Blacksberg, VA, Oct. 1988.

[14]Mook, D. T., and Nuhait, A. O., "Simulation of the Interaction Between Aerodynamics and Vehicle Dynamics in General Unsteady Ground Effect," Intersociety Advanced Marine Vehicles Conf., AIAA Paper 89-1498, Washington, DC, June 5–8, 1989.

[15]Mook, D. T., Roy, S., Choksi, G., and Dong, B., "Numerical-Simulation of the Unsteady Wake Behind an Airfoil," *Journal of Aircraft*, Vol. 26, No. 6, 1989, pp. 509–514.

[16]Konstadinopoulos, P., "A Vortex-Lattice Method for General Unsteady Subsonic Aerodynamics," M.S. Thesis, Dept. of Engineering Science and Mechanics, Virginia Polytechnic Inst. and State Univ., Blacksburg, VA, July 1981.

[17]Plotkin, A., and Kennel, C. G., "Thickness-Induced Lift on a Thin Airfoil in Ground Effect," *AIAA Journal*, Vol. 19, Nov. 1981, pp. 1484–1486.